Nano-sized TiO_2-Reinforced Natural Rubber Composites Prepared by Latex Compounding Method

Nabil Hayeemasae,[1] W.G.I.U. Rathnayake,[2] Hanafi Ismail[2]
[1]*Department of Rubber Technology and Polymer Science, Faculty of Science and Technology, Prince of Songkla University, Pattani Campus, 94000, Pattani, Thailand*

[2]*School of Materials and Mineral Resources Engineering, Engineering Campus, Universiti Sains Malaysia, 14300, Nibong Tebal, Penang, Malaysia*

This paper addresses nano-sized titanium dioxide (TiO_2) reinforced natural rubber composites. Micro-sized TiO_2 is simultaneously prepared to make a comparison with the composites containing nano-sized TiO_2. To improve the dispersion of TiO_2, this study also suggests a new method of incorporating TiO_2. Aqueous dispersions of micro- and nano-sized TiO_2 at the loadings of 0, 2, 4, 6, and 8 parts by weight per hundred parts of resin were dispersed in natural rubber latex, and then the resulting compounds were dried prior to mixing it with other ingredients on a two-roll mill. By applying this technique, the homogeneity of the compound is significantly improved. This can be clearly seen from the enhancement of tensile properties and morphological characteristics where the optimum loading was found at 6 parts by weight per hundred parts of resin of micro- and nano-sized TiO_2. Adding TiO_2 results in delayed scorch times and curing times wherein the curing process of filled compounds is shorter than the unfilled compound. J. VINYL ADDIT. TECHNOL., 00:000–000, 2015. © **2015 Society of Plastics Engineers**

INTRODUCTION

One of the most important phenomena in material science is the reinforcement of rubber by rigid particles, such as carbon black, silica, clays, and calcium carbonate, to name a few [1]. It is a well-known fact that the addition of rigid filler particles, even in small amounts, to an elastomer, strongly influences its mechanical behavior. Filler becomes the most important and second largest additive, followed by the base polymer in rubber compounding [2]. It is incorporated into a rubber compound to improve the physicomechanical properties and to make the final product more economical [3, 4]. Several studies reported on the substitution of white fillers, such as silica, calcium carbonate, and clay [5]. However, researchers have faced complications with the use of white fillers in elastomer composites. As for silica, it is mostly incompatible with elastomer, especially natural rubber. It requires an addition of compatibilizers or coupling agents, which complicates the processing method and subsequently increases production cost. Meanwhile, calcium carbonate and clay play major roles as non-reinforcing fillers, which result in deterioration of the mechanical properties [3–5]. Therefore, new filler materials need to be determined to maintain acceptable properties.

Titanium dioxide (TiO_2) is widely used as filler in many polymers because of the improved physical and mechanical properties it yields [6–8]. The nature of TiO_2 has great influence on the reinforcement of polymer composites. As reported by Meera et al. [9], TiO_2 particles do not possess any active hydroxyl groups on their surface, unlike silica particles that have available surface hydroxyl groups. This could provide a smaller tendency to form aggregate, which leads to a better dispersion of the TiO_2 accompanied with strong interfacial adhesion between matrix and filler in the polymer composites. The incorporation of TiO_2 in rubber composites was extensively studied by Saritha et al. [10]. It was found that the tensile strength, modulus, and tear strength increased with increasing TiO_2 loading. The relatively high elasticity modulus of TiO_2 was responsible for the mechanical gain of the composites. More recently, processing techniques were developed to allow the size of TiO_2 to decrease to nanoscale. Nano-sized TiO_2 was further studied in starch/(poly[vinyl alcohol]) blends by Sreekumar et al. [7]. It was observed that nano-sized TiO_2 could provide the composite superior mechanical properties because of the better interfacial adhesion between the polymer and filler. In another work by Seentrakoon et al. [11], it was reported that the efficient reinforcement of nano-sized TiO_2 originated from its larger surface. As a result, fine dispersion and homogeneous distribution of nano-sized TiO_2 in the rubber matrix were achieved.

Correspondence to: H. Ismail; e-mail: ihanafi@usm.my; profhanafi@gmail.com
DOI 10.1002/vnl.21497
Published online in Wiley Online Library (wileyonlinelibrary.com).

TABLE 1. The formulation used in this study.

Ingredients (phr)/ Sample codes	Gum	Micro TiO_2 (MT)	Nano TiO_2 (NT)
Natural rubber	100	100	100
ZnO	5	5	5
Stearic acid	2	2	2
CBS	0.5	0.5	0.5
IPPD	2	2	2
Sulfur	2.5	2.5	2.5
TiO_2	—	Variable (2, 4, 6, & 8)	Variable (2, 4, 6, & 8)

phr, parts by weight per hundred parts of resin; MT = Nano-sized TiO2; NT = Nano-sized TiO2; ZnO,; CBS, *N*-cyclohexyl-benzothiazyl-sulphenamide; IPPD, *N*−2-propyl-*N*′-phenylenediamine; TiO_2, titanium dioxide.

In this regard, nano-sized TiO_2 has received special interest as filler in the polymer matrices because of their specific properties. Currently, only a few works have been dedicated thoroughly to elastomer composites [9, 10]. Therefore, the aim of this work was to incorporate nano-sized TiO_2 in natural rubber composites together with the suggestion of a new route of dispersing TiO_2. Aqueous dispersion of nano-sized TiO_2 was mixed and dispersed in liquid dispersion of centrifuged natural rubber latex. The resulting compound was dried prior to mixing it with other ingredients on a two-roll mill. By applying this method, the homogeneity of the compound is expected to improve visibly. A comparative study on the curing and tensile and morphological properties of micro- and nano-sized TiO_2-filled natural rubber composites was also carried out.

EXPERIMENTAL

Materials

The formulation used in this study is listed Table 1. Low-ammonia-type centrifuged natural rubber latex (LATZ type), bentonite clay, and disodium 2,2′-methylene-*bis*-naphthalene sulphonate (Tamol^{TM}) were supplied by Zarm Scientific (M) Sdn. Bhd. (Penang, Malaysia). Micro-sized TiO_2 in 70% dispersion form was purchased from Aquaspersions (M) Sdn. Bhd. (Malaysia). The size of micro-TiO_2 is less than 3 μm with a density of 2.13 g/mL. Nano-sized TiO_2 was purchased from Sigma-Aldrich Co., LLC., with size ranging from 15 to 40 nm (as measured by transmission electron microscope [TEM]), 4.26 g/mL in density, surface area of 35–65 m^2/g Brunauer-Emmett Teller (BET), and more than 99.5% purity based on an analysis of trace materials [12]. Other compounding ingredients, such as zinc oxide, stearic acid, *N*-cyclohexyl-benzothiazyl-sulphenamide, *N*−2-propyl-*N*′-phenylenediamine, and sulphur, were purchased from Bayer (M) Ltd.

Preparation of the Composites

Figure 1 illustrates the diagram for the compounding preparation of natural rubber composites. The aqueous dispersion of nano-sized TiO_2 was prepared by using a mechanical ball mill. The compositions of 40 parts (w/w) of nano-sized TiO_2, 2 parts (w/w) of bentonite clay as a colloidal stabilizer, 1 part (w/w) of disodium 2,2′-methylene-*bis*-naphthalene sulphonate (Tamol^{TM}) as

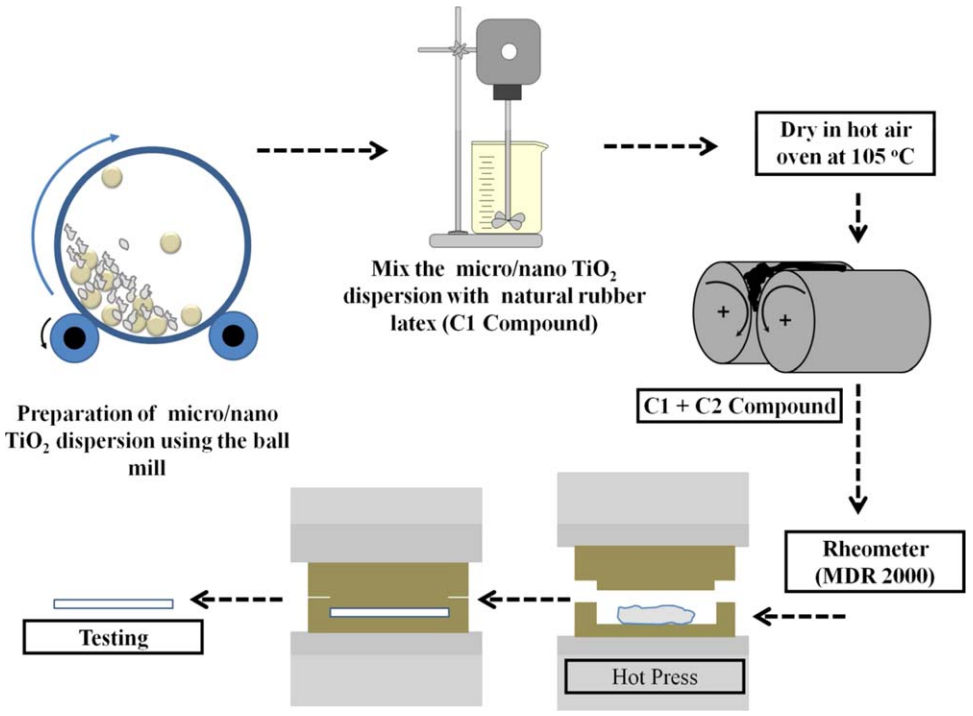

FIG. 1. Schematic illustration representing the preparation of the composites. [Color figure can be viewed in the online issue, which is available at wileyonlinelibrary.com.]

 DOI 10.1002/vnl

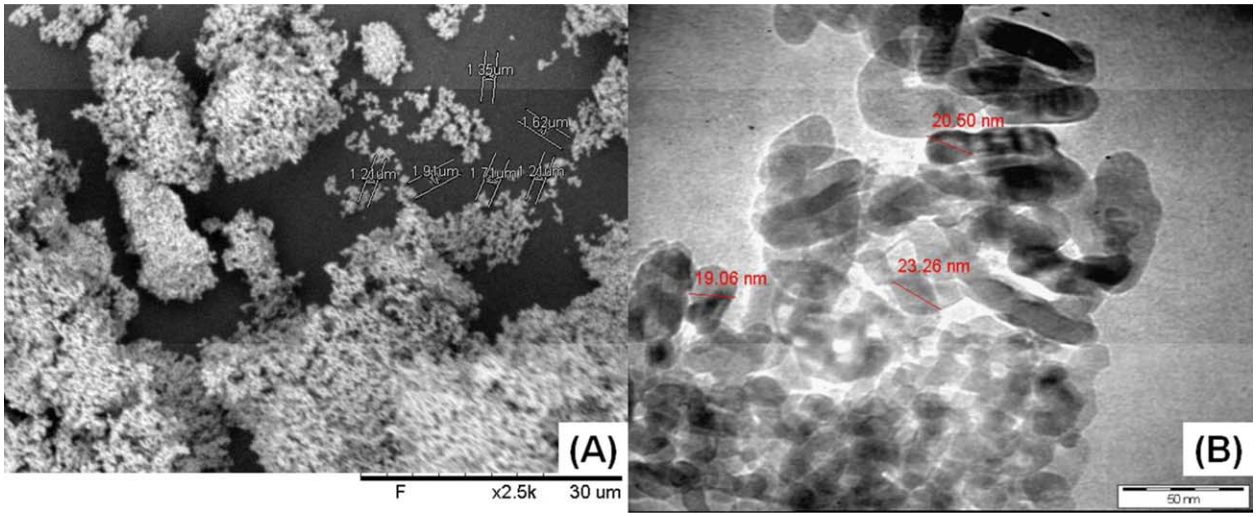

FIG. 2. SEM micrograph of TiO_2 microparticles at ×2,500 magnification (A) and TEM nanographs of TiO_2 nanoparticles at ×35,000 magnifications (B). [Color figure can be viewed in the online issue, which is available at wileyonlinelibrary.com.]

a dispersion agent, and 57 parts (w/w) of distilled water as the medium were added to the jar of the ball mill. Then, the whole mixture was kept on the ball-milling machine for 24 h at a rotation speed of 10 rpm. Later, the dispersion form of nano-sized TiO_2 was stored in an amber glass bottle to prevent photo-oxidation processing to take place.

The compounding preparation was done by mixing the centrifuged natural rubber latex with the aqueous dispersion of nano-sized TiO_2. The mixture was agitated mechanically for 8 h in order to ensure the homogeneity. Subsequently, this colloidal mixture was poured into a glass tray and dried in a hot air oven at 100°C for 8 h to remove all the water (C1 compound). Ultimately, the dried sheet of C1 compound was compounded with other additives on the laboratory size two-roll mill (Model XK-160). The final compound was later tested for its curing characteristics by using a Monsanto Moving Die Rheometer (MDR 2000). The compounds were subsequently compression-molded by using a stainless steel mold at 150°C with a pressure of 10 MPa using a laboratory hot-press based on the respective curing times. For the comparative studies, the unfilled natural rubber and micro-sized TiO_2-filled natural rubber composites were also prepared with the same procedure and formulation for comparing performance with those of nano-sized TiO_2-filled natural rubber composites.

Curing Characteristics

The curing characteristics of the natural rubber composites were obtained by using a Monsanto Moving Die Rheometer (MDR 2000), which was used to determine torques, scorch time (ts_2), and curing time (tc_{90}) according to ASTM D2084-11. Samples of the respective blends were tested at 150°C.

Measurement of Tensile Properties

Dumbbell-shaped samples were cut from the molded sheets according to ASTM D412-06ae2. Tensile tests were performed at a crosshead speed of 500 mm/min. Tensile tests were carried out with a universal tensile machine, Instron 3366, to determine the tensile properties such as tensile strength, elongation at break, stress at 100% (M100), and 300% (M300) elongation.

Scanning Electron Microscopy

The examination of tensile fractured surfaces was carried out by using scanning electron microscopes (SEMs), Hitachi Table Top Microscope, Model TM3000, and Zeiss Supra-35VP, respectively, to obtain information on the size of TiO_2 microparticles and possible presence of microdefects, respectively. An energy-dispersive X-ray spectroscope was coupled with the SEM and used to determine the elemental compositions in micro- and nano-sized filled natural rubber composites. The fractured pieces were coated with a layer of gold palladium to eliminate electrostatic charge build-up during examination.

Transmission Electron Microscope

The examination of nano-sized TiO_2 particles was carried out by using a TEM Philips Model CM12, and the images were analyzed by using Docu version 3.2 image analysis.

X-Ray Diffraction Analysis

The X-ray diffraction (XRD) analysis patterns of micro- and nano-sized TiO_2 composites were recorded by a Bruker AXS Model D8 diffractometer. The basal spacing of the TiO_2 before and after incorporating with

TABLE 2. Curing characteristics and tensile properties of micro- and nano-sized TiO_2-filled natural rubber composites.

Item	M_H (dN.m)	$M_H - M_L$ (dN.m)	ts_2 (min)	tc_{90} (min)	M100 (MPa)	M300 (MPa)	TS (MPa)	EB (%)
Gum	6.21	6.17	3.31	9.02	0.58 ± 0.01	1.33 ± 0.01	18.22 ± 1.52	1,198.8 ± 56.3
MT2	6.54	6.39	2.62	7.63	0.61 ± 0.03	1.37 ± 0.04	18.26 ± 0.78	1,132.6 ± 54.1
MT4	6.63	6.41	2.92	8.46	0.66 ± 0.01	1.47 ± 0.02	19.33 ± 0.23	1,053.4 ± 51.1
MT6	6.66	6.43	2.95	8.62	0.67 ± 0.02	1.49 ± 0.04	19.62 ± 0.97	1,045.4 ± 45.9
MT8	6.68	6.46	3.06	8.72	0.68 ± 0.01	1.52 ± 0.03	18.36 ± 1.70	1,044.0 ± 47.1
NT2	6.53	6.42	2.83	8.46	0.61 ± 0.01	1.37 ± 0.01	21.35 ± 1.15	1,145.0 ± 46.9
NT4	6.55	6.43	3.01	8.47	0.64 ± 0.01	1.45 ± 0.01	22.83 ± 0.81	1,139.2 ± 45.1
NT6	6.62	6.49	3.05	8.73	0.66 ± 0.01	1.50 ± 0.02	23.04 ± 0.36	1,116.0 ± 21.1
NT8	6.56	6.39	3.06	8.76	0.66 ± 0.02	1.51 ± 0.01	20.13 ± 0.88	1,054.0 ± 44.6

M_H, maximum torque; M_L,; ts_2, scorch time; tc_{90}, curing time; M100, modulus levels at 100%; M300, modulus levels at at 300%; Ts Tensile strength; EB Elongation at Break.

natural rubber was calculated by using Bragg's law. The CuK_α ($\lambda = 1.54060$ Å) was operated at 40 kV and 40 mA in combination with a Ni filter. The samples were scanned from $2\theta = 5$–$80°$ at the scanning rate of 0.001 θ/s.

RESULTS AND DISCUSSION

Morphology of Micro- and Nano-sized TiO_2 Particles

Figure 2A and B shows the SEM and TEM images of micro- and nano-sized TiO_2 particles, respectively. It can be clearly observed that nano-sized TiO_2 particles are far smaller than that of micro-sized TiO_2, indicating that high reinforcement can be attained by incorporating nano-sized TiO_2. It was also observed that TiO_2 microparticles are irregular shaped, whereas TiO_2 nanoparticles are rod-shaped or elongated.

Curing Characteristics

The curing characteristics of micro- and nano-sized TiO_2-filled natural rubber composites are tabulated in Table 2. The addition of TiO_2 resulted in delayed scorch (ts_2) and curing times (tc_{90}). Increased TiO_2 loading results in a shorter curing process than gum vulcanizate. The ts_2 and tc_{90} are the measures of premature vulcanization and the optimum vulcanization process of the composites [13]. It was also observed that the ts_2 and tc_{90} of nano-sized TiO_2-filled natural rubber composites were slightly longer than micro-sized TiO_2-filled composites. In general, a slower cure rate is obtained when fillers have a high surface area [3]. This causes retardation of the accelerator activity, which slows down the sulfur vulcanizing reaction, leading to increased ts_2 and tc_{90}. Maximum torque (M_H) is a measurement of the stiffness or shear modulus of completely vulcanized test specimens at the curing temperature.

In addition, M_H increased consistently with the increase of micro- and nano-sized TiO_2. Increments of M_H correlated to increasing TiO_2 loading were due to the TiO_2 itself. It highly restricts molecular motion of macromolecules and tends to reduce resistance to flow [14]. Similar observations were also made for torque difference ($M_H - M_L$), which is a measure of the difference between the stiffness or shear modulus of a fully vulcanized and the nonvulcanized test specimen taken at the lower point of the vulcanizing curve. At a similar loading rate of TiO_2, the M_H and $M_H - M_L$ of micro-sized TiO_2-filled natural rubber composites were slightly higher than that of nano-sized TiO_2-filled natural rubber composites. These properties correlate to the stiffness of the fillers. TiO_2 nanoparticles used in this study are rod-shaped or elongated (see Fig. 2B), which have high surface and contact areas that soften the composites. The incorporation of nano-sized TiO_2 in natural rubber does not affect the volume of the deformable phase, as is the case with micro-sized TiO_2-filled natural rubber composites. As a consequence, when nano-sized TiO_2 counterparts are submitted to shear force, the actual deformation was much lower because of higher deformable volumes than that of micro-sized TiO_2, leading to lower the M_H and $M_H - M_L$.

Tensile Properties

Modulus levels at 100% (M100) and 300% (M300) elongation are listed in Table 2. M100 and M300 increased gradually with increasing micro- and nano-sized TiO_2 loading. As more TiO_2 particles are incorporated into the rubber, the elasticity of the rubber is reduced, resulting in more rigid, stiffer, and harder vulcanizates. Furthermore, the increments of tensile modulus of both composites are due to the effect of strain amplification. This is most likely because both micro- and nano-sized TiO_2 is in a rigid phase at the tested temperature, which cannot be deformed. Subsequently, the intrinsic strain of the polymer matrix is higher than the external strain, yielding a strain-independent contribution to the modulus, well-known as the hydrodynamic effect [1, 2]. However, this phenomenon is not found using nano-sized TiO_2-filled natural rubber composites. At any given loading rate, the nano-sized TiO_2-filled natural rubber composites show a slightly higher tensile modulus than that of the micro-sized TiO_2-filled natural rubber composites. This is

 DOI 10.1002/vnl

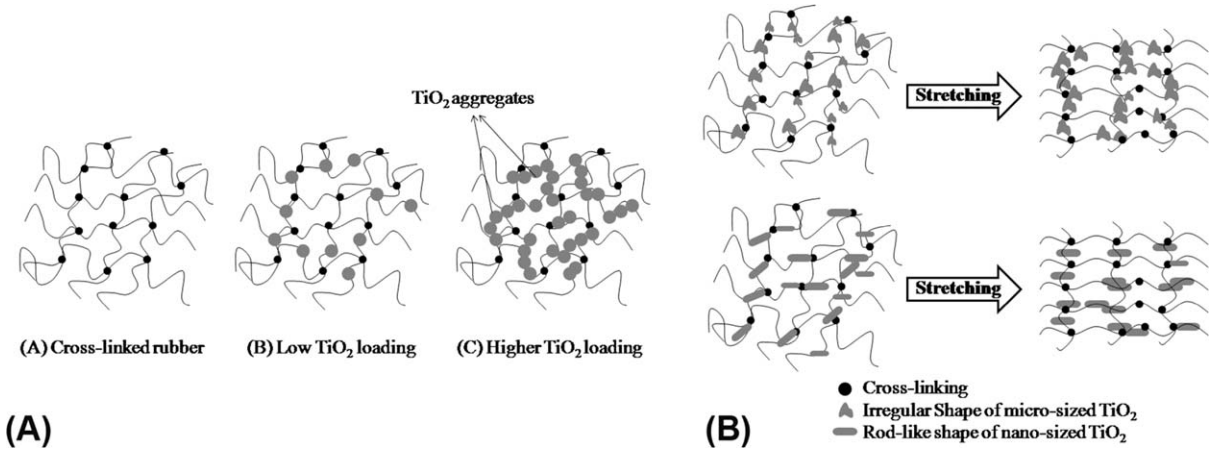

FIG. 3. Schematic illustrations representing the gum and filled vulcanizates (a) and the nature of micro- and nano-sized TiO_2 on stretching (b).

due to the smaller size of nano-sized TiO_2, resulting in a lower intrinsic strain, therefore lowering the tensile modulus. Fu et al. [15] elucidated another relevant reason that the modulus is also related to the hardness of the filler itself. As seen in Fig. 2A and B, nano-sized TiO_2 is rodlike in shape, so it softens the composites and lowers the stiffness of the rubber composites. Similar observations were described elsewhere [16–18], suggesting that the modulus of composites is not only influenced by filler's particle size.

Table 2 also represents the tensile strength of micro- and nano-sized TiO_2-filled natural rubber composites. The tensile strength increased up to 6 parts by weight per hundred parts of resin (phr) of TiO_2; above this level, strength was reduced. TiO_2 has a relatively high elastic modulus, so it is frequently combined with various polymers to increase the mechanical gain in composites. The particle size of the filler is smaller than other macroscopic fillers [10], which results in a better interaction between the natural rubber matrix and the filler. Another probable reason is the new compounding technique, proposed in the preceding section. Applying this technique resulted in superior tensile strength in both composites to gum vulcanizate. Well-dispersed TiO_2 is strongly responsible for the improvement of stress transfer between the matrix and the filler. It was also found that nano-sized TiO_2-filled natural rubber composites have a higher tensile strength than that of micro-sized TiO_2 counterparts. The surface area is one of the important characteristics in reinforcing fillers because the particles with larger surface areas increase the properties of the polymer [19, 20]. Stronger bonding occurs with more contact area available to react with the polymer matrix. The enhancement of this interaction improves the wetting and adhesion of the polymer to the filler and consequently allows better stress transfer in the composites.

The reduction in tensile strength with loading beyond 6 phr of TiO_2 loading is simply due to the dilution effect [21]. When more TiO_2 particles are integrated into the natural rubber matrix, the TiO_2 particles tend to interact with each other, known as filler–filler interaction. Another reason is the incompetence of TiO_2 particles to encourage stress transfer from the elastomeric phase and the agglomeration of TiO_2 particles, which is seen in the results of micrographs in the latter section. The elongation at break of the composites is summarized in Table 2. Increased TiO_2 loading results in a reduction of deformability of rigid interfaces between the TiO_2 particles and the rubber matrix [6, 13]. At a similar TiO_2 loading, the nano-sized TiO_2-filled natural rubber composites showed higher levels of elongation at break. The larger surface area and the softer characteristic of nano-sized TiO_2 loaded material lead to better interfacial interactions between nano-sized TiO_2 and natural rubber. The homogenous dispersion of nano-sized TiO_2 inside the natural rubber obtained from latex mixing is responsible for the higher ductility of the composites.

The reinforcement of TiO_2-filled natural rubber composites can be further explained by its proposed mechanisms, as depicted in Fig. 3A and B. At low TiO_2 loading, the chances of forming aggregates are comparatively less and hence good dispersion of the filler is achieved. Therefore, the stress transfer rate is almost comparable with that of the gum vulcanizate, as shown in Fig. 3A. However, at higher TiO_2 loading, due to the breakdown of the aggregates, the stress transfer rate becomes ineffective. In the case of the highly filled system [9], the rubber chains get physically adsorbed on the filler surface, and there are multiple points of attachments of rubber chains at the filler surface as shown in the schematic. With the breakdown of the aggregates, the rubber chains get desorbed from the filler surface and hence the tensile strength and elongation at break decreased.

Figure 3B illustrates the schematic representing how the micro- and nano-sized TiO_2 behave when certain stretching is applied. As mentioned earlier, because of the elongated or rodlike morphology and unique structure of nano-sized TiO_2, it can be homogeneously dispersed in the natural rubber matrix. After applying the strain, nano-sized TiO_2 tends to rearrange and help to promote better

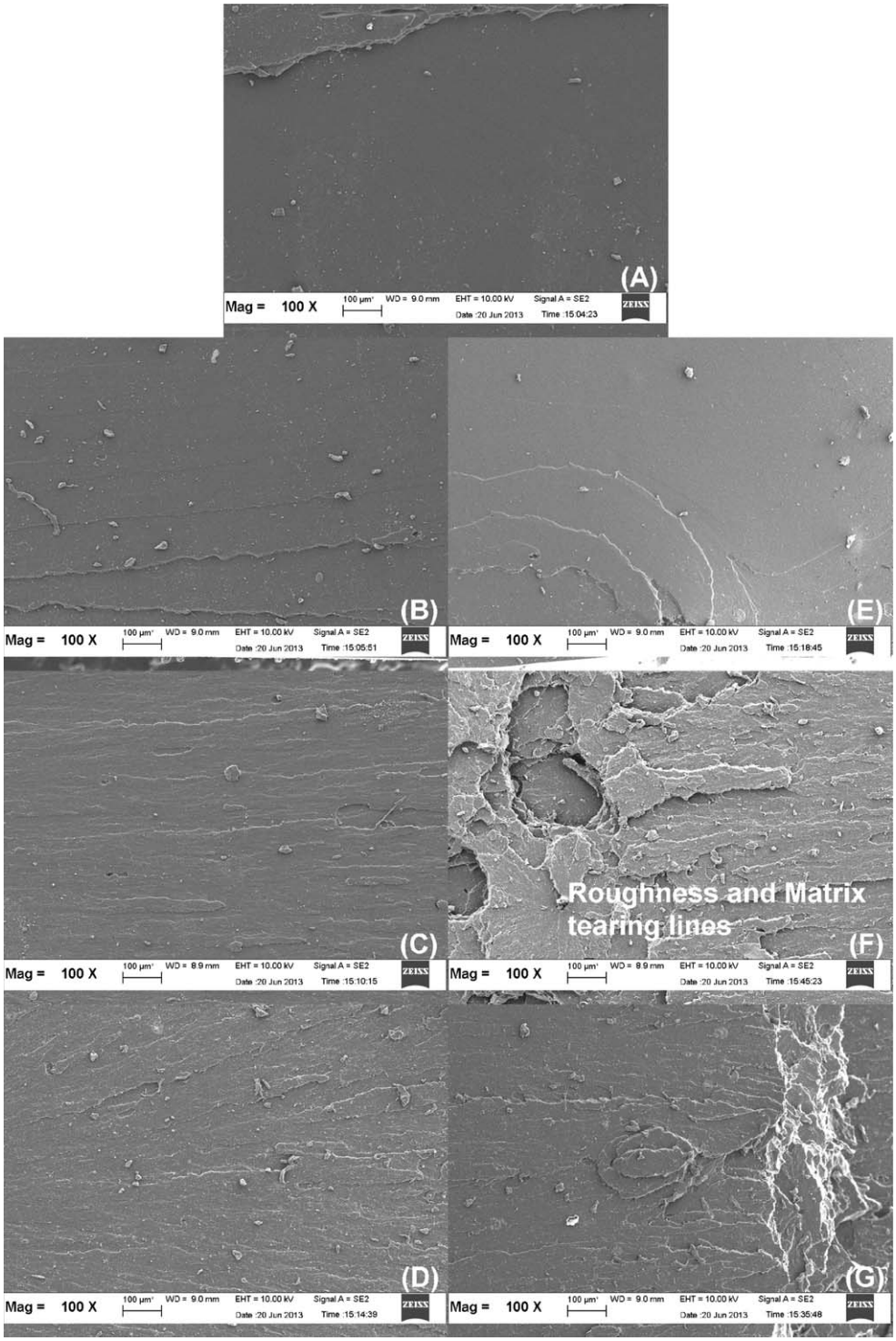

FIG. 4. Tensile fractured surfaces at ×100 magnification of micro- and nano-sized TiO_2-filled natural rubber composites: gum (a); MT2 (b); MT6 (c); MT8 (d); NT2 (e); MT6 (f); NT8 (g).

stress transfer from rubber matrix to the filler. On the contrary, the rearrangement of micro-sized TiO_2 is not well-observed on stretching due to its bigger size and irregular shape, and the aggregation is comparatively more pronounced. As a consequence, the tensile strength is lower than those of nano-sized TiO_2-filled natural rubber composites.

Microfractured Surfaces

Figure 4 illustrates the SEM micrographs of tensile fractured surfaces in micro- and nano-sized TiO_2-filled natural rubber composites at ×100 magnification. Figure 4A shows the fractured surfaces of gum vulcanizate. Smooth and soft surfaces were observed because no rigid

 DOI 10.1002/vnl

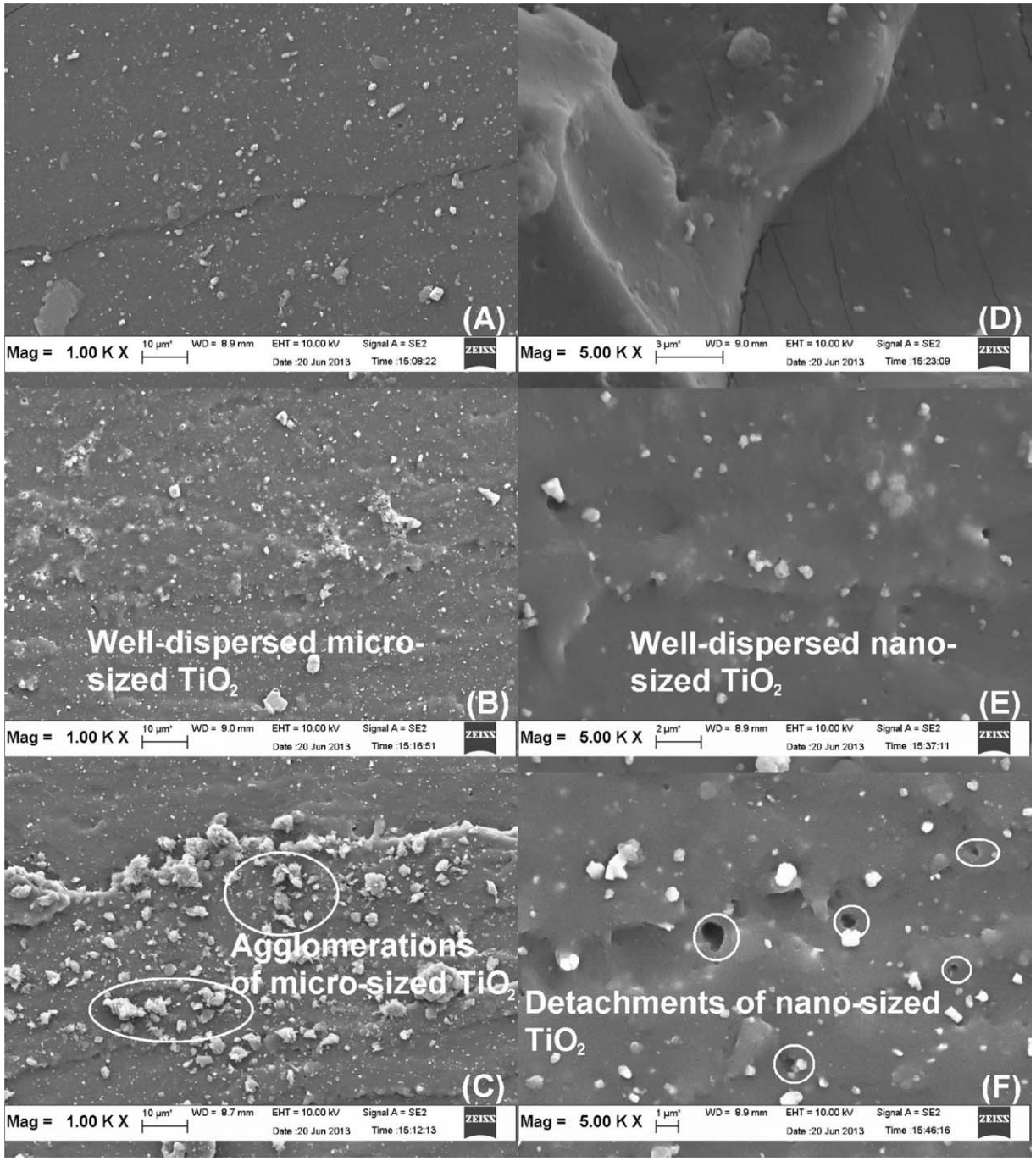

FIG. 5. Tensile fractured surfaces of micro-sized TiO_2-filled natural rubber composites (×1,000 magnifications) at the loading of 2 phr (A), 6 phr (B), and 8 phr (C) and nano-sized TiO_2-filled natural rubber composites (×5,000 magnification) at loadings of 2 phr (D), 6 phr (E), 8 phr (F).

filler was incorporated into the matrix. Figure 4B, C, and D shows the fractured surfaces of micro-sized TiO_2-filled natural rubber composites at 2, 6, and 8 phr. The roughness and frequency of tearing in micro-sized TiO_2-filled natural rubber composites were visible when TiO_2 was added into the matrix. This indicates that more energy is needed to break the sample. A slight increment in the matrix's roughness with increased levels of micro-sized TiO_2 is in agreement with the tensile results observed. The tensile fractured surfaces of the nano-sized TiO_2-filled natural rubber composites are illustrated in Fig. 4E, F, and G. With the addition of nano-sized TiO_2 in concentrations up to 6 phr, an augmentation in surface roughness occurs as well as a homogeneous pattern similar to the fractured surface with loading beyond 6 phr (Fig. 4G) and materials with gum vulcanizate (Fig. 4A), which shows less tearing lines leading to lower ultimate tensile value. Better homogeneity in nano-sized TiO_2-filled natural rubber composites indicates a coherence of the nano-TiO_2 molecules and the natural rubber phases. The uniform dispersion of TiO_2 in the natural rubber matrix alters the crack path, which leads to resistance from crack

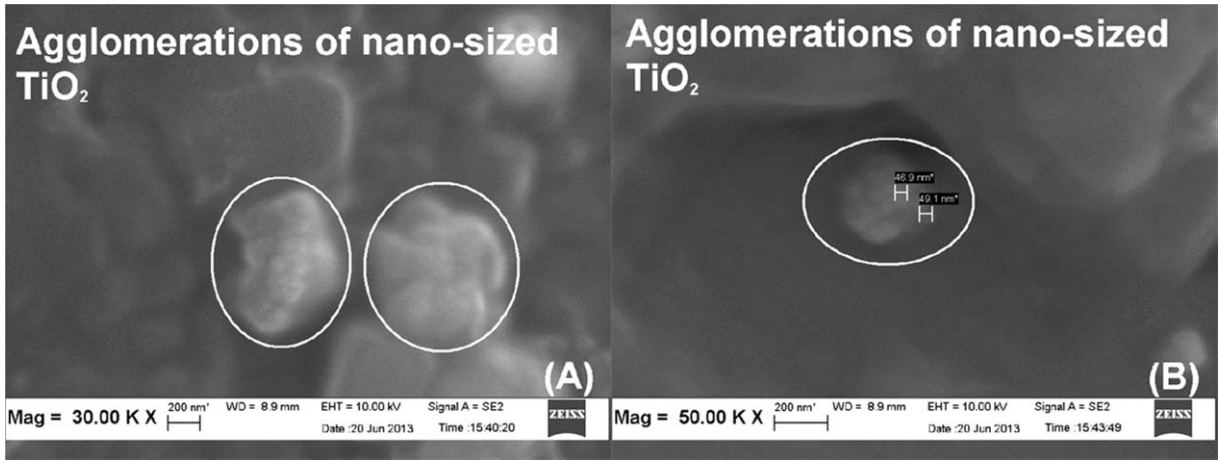

FIG. 6. The agglomerations development of 8 phr of nano-sized TiO_2 at ×30,000 (A) and ×50,000 (B) magnifications.

propagation and hence results in higher tensile strengths and improved mechanical properties. Similar observations have been reported on the changes of fractured surfaces with the addition of fillers in natural rubber composites [22–24].

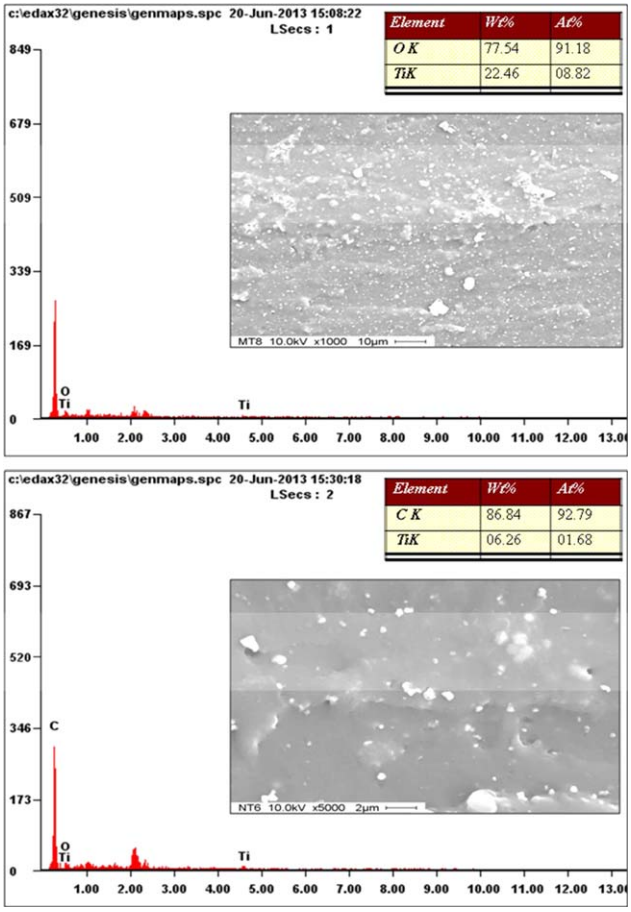

FIG. 7. Elemental analysis of micro- and nano-sized TiO_2-filled natural rubber composites: MT8 at ×1,000 magnifications (top) and NT6 at ×5,000 magnifications (bottom). [Color figure can be viewed in the online issue, which is available at wileyonlinelibrary.com.]

Figure 5A–F shows the filler dispersion of micro- and nano-sized TiO_2-filled natural rubber composites at high magnifications. As seen in Fig. 5A and B, the micro-sized TiO_2 was dispersed homogenously in the rubber matrix, suggesting that using the new route for preparing the composites results in better dispersion. The homogeneity of the composites are significantly improved, especially with loading up to 6 phr. Well-dispersed micro-sized TiO_2 is responsible for the improved tensile strength. Similar observations are found with nano-sized TiO_2-filled natural rubber composites (see Fig. 5D and E). However, when micro- and nano-sized TiO_2 are incorporated beyond 6 phr, the TiO_2 tends to agglomerate, due to the strong filler–filler interaction as well as the detachment of nano-sized TiO_2. This is shown in Fig. 5C and F, respectively, indicating that less energy is required to cause failure in the materials. Figure 6A and B shows the agglomerations of nano-sized TiO_2 in the rubber matrix at higher magnifications. The high filler–filler interaction of TiO_2 in natural rubber matrices causes a reduction of tensile strength. Figure 7 shows an elemental analysis by energy dispersive X-ray analysis and the presence of micro- and nano-sized TiO_2-filled natural rubber composites. It is clear that the prominent peak was due to elemental TiO_2 adsorbed into the natural rubber matrix.

X-Ray Diffraction Analysis

XRD analysis is a well-known analysis technique used to determine crystal sizes and structure [25, 26]. This technique is used to prove the presence of elements inside natural rubber–based samples. In this study, it was applied to analyze the presence of micro- and nano-sized TiO_2-filled natural rubber composites. As shown in Fig. 8A, the XRD peak pattern of the rubber samples modified by micro-sized TiO_2 shows that the sample consists of both ZnO and TiO_2 elements. The presence of ZnO is due to its use as an activator in rubber compounding (see Table 1). Thus, the reference pattern matches the

 DOI 10.1002/vnl

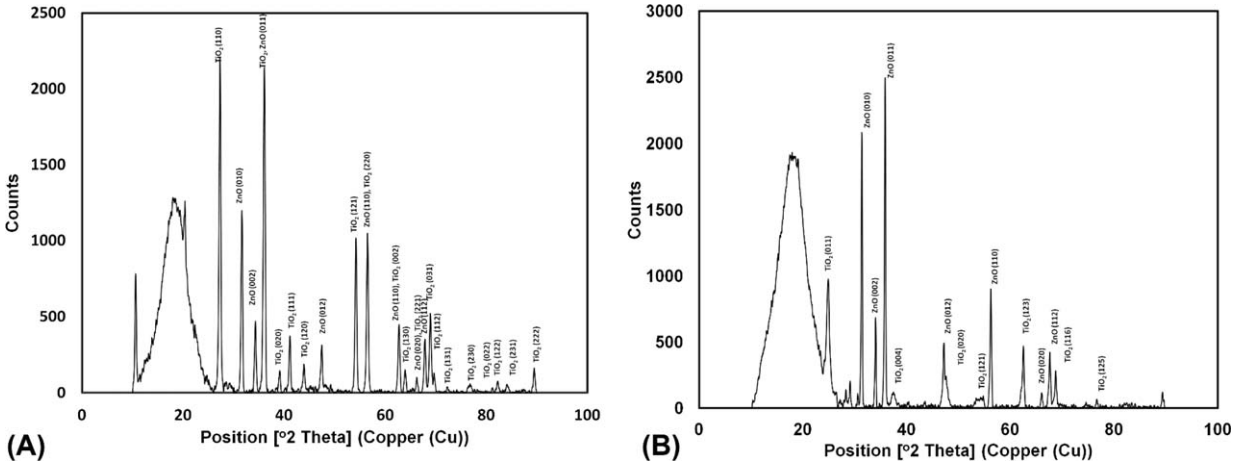

FIG. 8. XRD pattern of micro-sized TiO_2 (a) and nano-sized TiO_2 and (b) filled natural rubber composites.

reference code, 98-005-5014, which is the hexagonal phase of ZnO.

As shown in the XRD pattern, some peaks are from TiO_2, which is the rutile phase of TiO_2. Those peaks are a perfect match to the reference code 98-007-6757, which is for the tetragonal phase of TiO_2. The crystallite size was 242.2 Å. The nano-sized filled composite has a different peak pattern than the micro-sized filled composite, as seen in Fig. 8B. The peaks in the XRD match both ZnO and TiO_2 elements. The ZnO peaks are similar to the micro-sized TiO_2-filled composite. However, the peaks do not match in the same phases of TiO_2 as those detected in the micro-sized TiO_2-filled composite. The peaks of TiO_2 in the nano-sized TiO_2-filled composite are a perfect match to the anatase phase, reference code 98-006-6624. The crystal system for this anatase type TiO_2 is tetragonal and the crystallite size is 118.3 Å. As explained by Ahmad et al. [27], the anatase type TiO_2 is the most versatile nano-sized TiO_2 and is commonly used in research for photocatalytic activities [27]. The two different XRD patterns from the modified samples using nano-sized TiO_2 show different peak patterns, different crystal structures, and different crystallite size. This is good evidence that the nano-sized TiO_2-filled natural rubber composites consist of the Anatase-type tetragonal crystal system and have very small crystallites.

CONCLUSIONS

The following conclusion can be presented:

1. SEM and TEM images of micro- and nano-sized TiO_2 particles clearly showed that nano-sized TiO_2 particles are rod-shaped or elongated, which are smaller than that of micro-sized TiO_2, indicating that high reinforcement can be attained by incorporating nano-sized TiO_2.
2. The addition of TiO_2 resulted in delayed scorch (ts_2) and curing times (tc_{90}) where it was shorter than that of gum vulcanizate. M_H increased consistently with the increase of micro- and nano-sized TiO_2 due to the highly restricted molecular motion of macromolecules when TiO_2 was incorporated.
3. The tensile strength of nano-sized TiO_2-filled natural rubber composites is superior to micro-sized TiO_2-filled natural rubber composites where the optimum tensile strength was found at 6 phr of micro- and nano-sized TiO_2.
4. Nano-sized TiO_2-filled composites exhibited better dispersion, shown clearly by SEM micrographs. As for XRD patterns, the peak patterns, crystal structures, and crystallite size were differently found in both micro- and nano-sized TiO_2-filled natural rubber composites.

ACKNOWLEDGMENTS

W.G.I.U. Rathnayake would like to acknowledge Universiti Sains Malaysia (USM) for the Post-Doctoral Fellowship.

REFERENCES

1. H. Nabil, H. Ismail and A.R. Azura, *J. Vinyl Addit. Technol.*, **18**, 139 (2012).
2. J. Zhang, L. Wang and Y. Zhao, *Mater. Design*, **50**, 322 (2013).
3. H. Nabil, H. Ismail and A.R. Azura, *J. Elast. Plast.*, **43**, 429 (2011).
4. R.V. Sheril, M. Mariatti and P. Samayamutthirian, *J. Vinyl Addit. Technol.*, **20**, 160 (2014).
5. A.H. Navarchian, M. Joulazadeh and S. Mousazadeh, *J. Vinyl Addit. Technol.*, **19**, 276 (2013).
6. A. Buzarovska, *Polym.-Plast. Technol. Eng.*, **52**, 280 (2013).
7. P. Sreekumar, M.A. Al-Harthi and S.K. De, *J. Compos. Mater.*, **46**, 3181 (2012).
8. J. Ahmad, K. Deshmukh and M.B. Hägg, *Int. J. Polym. Anal. Charact.*, **18**, 287 (2013).
9. A.P. Meera, S. Said, Y. Grohens, A.S. Luyt and S. Thomas, *Ind. Eng. Chem. Res.*, **48**, 3410 (2009).
10. A. Saritha, K. Joseph, A. Boudenne and S. Thomas, *Polym. Compos.*, **32**, 1681 (2011).
11. B. Seentrakoon, B. Junhasavasdikul and W. Chavasiri. *2013. Polym. Degrad. Stab.*, **98**, 566 (2013).
12. Technical Report of Sigma-Aldrich (M) Sdn. Bhd. (2015) http://www.sigmaaldrich.com/Graphics/COfAInfo/Sigma

SAPQM/SPEC/71/718467/718467-BULK_____ALDRICH_.pdf [accessed on May 14, 2015].
13. C. Nakason, A. Kaesaman, and K. Eardrod, *Mater. Lett.*, **59**, 4020 (2005).
14. H. Nabil and H. Ismail, *Int. J. Polym. Anal. Charact.*, **19**, 159 (2014).
15. S.-Y. Fu, X.-Q. Feng, B. Lauke, and Y.-W. Mai, *Compos Part B: Eng.*, **39**, 933 (2008).
16. F. Lange and K. Radford, *J. Mater. Sci.*, **6**, 1197 (1971).
17. K. Radford, *J. Mater. Sci.*, **6**, 1286 (1971).
18. J. Spanoudakis and R. Young, *J. Mater. Sci.*, **19**, 473 (1984).
19. S. Palaniandy, N.A. Kadir, and M. Jaafar, *Miner. Eng.*, **22**, 695 (2009).
20. S.S. Idrus, H. Ismail, and S. Palaniandy, *Polym. Test.*, **30**, 251 (2011).
21. S. Poompradub, Y. Ikeda, Y. Kokubo, and T. Shiono, *Eur. Polym. J.*, **44**, 4157 (2008).
22. H. Ismail, P. Pasbakhsh, M. Fauzi, and A. Abu Bakar, *Polym. Test.*, **27**, 841 (2008).
23. H. Ismail and S. Shaari, *Polym. Test.*, **29**, 872 (2010).
24. S. Kanking, P. Niltui, E. Wimolmala, and N. Sombatsompop, *Mater. Design*, **41**, 74 (2012).
25. H. Stanjek and W. Häusler, *Hyper. Interact.*, **154**, 107 (2004).
26. W. Rathnayake, H. Ismail, and A. Baharin, *J. Appl. Polym. Sci.*, **131**, 1 (2014).
27. D.A. Ahmad, G.H. Awan, and S. Aziz, "Synthesis and Applications of TiO_2 Nanoparticles, Pakistan Engineering Congress," in *70th Annual Session Proceedings*, 404 (2006).

 DOI 10.1002/vnl